Dissociating Mechanisms That Underlie Seasonal and Developmental Programs for the Neuroendocrine Control of Physiology in Birds

[iD]Timothy Adam Liddle,[1] Gaurav Majumdar,[2] Calum Stewart,[1] Maureen M. Bain,[1] and Tyler John Stevenson[1]

[1]Laboratory of Seasonal Biology, School of Biodiversity, One Health, and Veterinary Medicine, University of Glasgow, Glasgow, United Kingdom and [2]Department of Zoology, University of Allahabad, Allahabad, India

Abstract

Long-term programmed rheostatic changes in physiology are essential for animal fitness. Hypothalamic nuclei and the pituitary gland govern key developmental and seasonal transitions in reproduction. The aim of this study was to identify the molecular substrates that are common and unique to developmental and seasonal timing. Adult and juvenile quail were collected from reproductively mature and immature states, and key molecular targets were examined in the mediobasal hypothalamus (MBH) and pituitary gland. qRT-PCR assays established deiodinase type 2 (*DIO2*) and type 3 (*DIO3*) expression in adults changed with photoperiod manipulations. However, *DIO2* and *DIO3* remain constitutively expressed in juveniles. Pituitary gland transcriptome analyses established that 340 transcripts were differentially expressed across seasonal photoperiod programs and 1,189 transcripts displayed age-dependent variation in expression. Prolactin (*PRL*) and follicle-stimulating hormone subunit beta (*FSHβ*) are molecular markers of seasonal programs and are significantly upregulated in long photoperiod conditions. Growth hormone expression was significantly upregulated in juvenile quail, regardless of photoperiodic condition. These findings indicate that a level of cell autonomy in the pituitary gland governs seasonal and developmental programs in physiology. Overall, this paper yields novel insights into the molecular mechanisms that govern developmental programs and adult brain plasticity.

Key words: Coturnix japonica; MBH; Oxford Nanopore RNA sequencing; photoperiod; pituitary gland; seasonality

Significance Statement

Seasonal physiology is pervasive in the animal kingdom. While much is known regarding how the brain perceives annual changes in daylength (also referred to as photoperiod) and dynamics of the neuroendocrine control of seasonal physiology in adult animals, studies in juveniles are limited. Here, we assess genome-wide and targeted transcriptomic changes in the pituitary gland, a key brain region connecting photoreception with physiological plasticity in adult and juvenile Japanese quail. The analyses identified several novel transcripts that are correlated with photoperiod- and developmental programs in seasonal physiology. The findings demonstrate a level of pituitary gland cell specificity for the regulation of both development and reproductive fitness that is dependent on both age and experienced photoperiod.

Introduction

Seasonal and developmental programs in the neuroendocrine control of reproductive physiology in mammals and birds are well characterized (Stevenson et al., 2012a,b;

Plant, 2015; Stevenson et al., 2017). However, very few studies have directly compared the similarities and differences in how the hypothalamus governs these long-term changes in physiology. Animals in temperate regions experience variable environmental conditions within and across seasons, including changes in daylength, ambient temperature, and availability of food (Sharp, 1996; Hau, 2001). The annual change in daylength, referred to as photoperiod, is a powerful signal that animals use as a predictive cue to anticipate environmental conditions ideal for breeding (Bradshaw and Holzapfel, 2007; Wood and Loudon, 2014; Payton et al., 2017; Stevenson et al., 2022). In most mammals, the nocturnal duration of melatonin secretion from the pineal gland provides a physiological code of photoperiod and drives many molecular, cellular, and morphological changes in the median eminence and pituitary gland (Wood and Loudon, 2014; Stevenson et al., 2022). Conversely, birds have photoreceptors located deep in the hypothalamus that directly detect light stimulation to drive photoperiod-induced changes in seasonal physiology (Stevenson and Ball, 2012; Pérez et al., 2019, 2023; Liddle et al., 2022). Despite these markedly different neuroendocrine control mechanisms, the pituitary gland is a conserved anatomical structure that provides the essential gating mechanism to permit and inhibit communication from the hypothalamus to peripheral tissues (e.g., gonads).

Juvenile animals have a heightened sensitivity to the effects of photoperiod on reproductive physiology. Siberian hamsters raised in long summer-like photoperiods initiate puberty at approximately postnatal day 21 (Spears et al., 1990). Transfer of hamsters to short winter-like photoperiods induces a rapid inhibition of gonadal development resulting in gonadal involution in <7 d (Prendergast et al., 2004). A single subcutaneous injection of melatonin to weaned hamsters (i.e., postnatal day 18) is sufficient to prevent gonadal growth, despite being housed in stimulatory long photoperiods (Prendergast et al., 2013). Similarly, Japanese quail reared in long stimulatory photoperiods reach sexual maturity by 28–35 d posthatch (Follett, 1976). Birds that are transferred to shorter photoperiods (e.g., 12 light, 12 dark) delay gonadal growth by up to 2 weeks (Follett and Maung, 1978), and photoperiods <12 h light completely prevent reproductive maturation (Follett and Sharp, 1969; Abdelnabi and Ottinger, 2003).

Only a few studies have examined how photoperiod manipulations early in development impact the neuroendocrine regulation of reproductive physiology. In adult birds and mammals, the expression of deiodinase enzymes, deiodinase type 2 (*DIO2*) and deiodinase type 3 (*DIO3*), is a molecular signature of a photoperiodic state (Nakane and Yoshimura, 2014; Rani and Kumar, 2014). Long photoperiods increase *DIO2* expression, which catalyzes the conversion of inactive thyroxine (T4) into active triiodothyronine (T3), and short photoperiods initiate the reversal by stimulating *DIO3* expression and reducing hypothalamic triiodothyronine (Yoshimura et al., 2003; Barrett et al., 2007). In juvenile Siberian hamsters, transfer to short photoperiods or subcutaneous injections of melatonin rapidly increases *DIO3* expression in the mediobasal hypothalamus (MBH; Prendergast et al., 2013; Sáenz de Miera et al., 2017). Whether similar rapid changes occur in juvenile birds is currently unknown. Resolving whether *DIO3* or *DIO2* display an augmented sensitivity to photoperiodic cues early in development is important to develop our understanding of conserved neuroendocrine pathways that underlie photoperiod and developmental programming of seasonal physiology.

Seasonal and reproductive maturation requires the release of gonadotropin-releasing hormone (*GnRH*) into the hypophyseal portal system, allowing for transport into the pituitary gland where GnRH acts on gonadotrophs to stimulate the release of luteinizing hormone (*LH*) and follicle-stimulating hormone (*FSH*; Stevenson et al., 2012a,b). Therefore, the pituitary gland can be viewed as the final mediator between seasonal and developmental programming of seasonal physiology. The objectives of this study were twofold. First, the expression profiles of *DIO2* and *DIO3* in the MBH tissue were examined in adult and juvenile Japanese quail held in long or short photoperiods. The findings indicate neither *DIO2* nor *DIO3* show a similar pattern in adults compared with juveniles suggesting a clear dissociation between developmental programming and seasonal photoperiodic regulation of deiodinase expression. The second objective was to identify seasonal and developmental programmed changes in the pituitary gland. Oxford Nanopore RNA sequencing was conducted to produce a pituitary transcriptome and enable a comprehensive overview of age- and light-dependent molecular changes. The data described herein suggest cellular specificity in how the pituitary gland controls long-term programs in physiology.

Materials and Methods

Animals and ethical permissions. Japanese quail were purchased from MoonRidge Farms, Exeter. Five-week-old male quail ($n = 12$) were housed on a 16 L:8 D (L, light; D, dark) light schedule. All birds were provided Farmgate layers pellets and tap water *ad libitum*. Two-day-old Japanese quail eggs ($n = 40$) were placed in an incubator (Brinsea OVA Easy Advance 380; temperature, 37.5°C; relative humidity, 50–60%) until hatching (16–18 d). Hatched chicks ($n = 8$ males, $n = 3$ females) were moved to quail pens provided with heat lamps (37.5°C) and provided blended Heygates Superstarter Crumb and tap water *ad libitum*. Animal research was conducted according to the ARRIVE guidelines and Home Office–approved project and establishment licenses. All animal procedures were performed in accordance with the relevant establishment's animal care committee regulations.

Experimental design. Five-week-old birds were acclimated to a long photoperiod for 2 weeks. Then birds were placed on nonstimulatory photoperiods to induce gonadal involution and collected in short days (8 L) after 8 weeks. A subset of the short-day birds ($n = 6$) was humanely killed using cervical dislocation followed by decapitation. Another group ($n = 6$) was placed on stimulatory photoperiods to induce gonadal growth and collected in a long photoperiod after 8 weeks.

Newly hatched juveniles were acclimated to a long photoperiod for 5 d. Birds were divided into two groups pseudorandomly assigned in either a long (16 L, $n = 6$) or short photoperiod (8 L, $n = 5$) for 5 d. The 16 L juvenile group contained four males and two females, whereas the 8 L juvenile group contained four males and one female. On posthatch day 10, chicks were killed by cervical dislocation followed by decapitation. For all birds, brain and pituitary tissues were frozen on dry ice and stored at −70°C. During collections, the pituitary stalk was severed, leaving the pars tuberalis attached to the MBH. Pituitary tissue including the pars distalis, retained for both qRT-PCR analyses and sequencing, was dissected from the sella turcica. Testis length was measured using calipers to the nearest 0.01 mm. Ovary length of the three female chicks was measured to confirm the photoperiod state. Birds were assigned a fat score from 0 to 5 based on a scale established in white-crowned sparrows (Wingfield and Farner, 1978).

Whole-brain dissections. To isolate the MBH/hypothalamic regions, a brain matrix was used within a cryostat chamber. Previously published anatomical coordinates acted as guidance for dissection (Nakao et al., 2008; Stevenson et al., 2012a,b). Brains were positioned ventral side up and oriented with the caudal direction facing upward. The MBH was dissected using a brain matrix. First, a 3 mm coronal section from the optic chiasm in a posterior direction was performed. Then 2 mm lateral cuts and a 2 mm dorsal cut were conducted to isolate the MBH. This dissection protocol reliably isolates the MBH in Japanese quail (Majumdar et al., 2023). Brains were then returned to −70°C.

RNA extraction and cDNA synthesis. For all samples, RNA was extracted using TRIzol reagent following the manufacturer's protocol. RNA was then purified using an RNEasy MinElute cleanup kit (Qiagen). RNA quality and purity were measured with NanoDrop ND-100 (NanoDrop Technologies). Both pituitary gland and hypothalamic RNA were retained for cDNA synthesis and qRT-PCR analyses; however, some pituitary gland RNA were also retained for direct use in RNA sequencing. cDNA was synthesized from TRIzol-extracted RNA using a reaction mixture containing 4 µl ~50 ng/µl total RNA (~200 ng total), 2 µl 5× first-strand buffer (Thermo Fisher Scientific), 1 µl DTT (10 mM), 0.2 µl 20 mM random primers (Promega), 0.2 µl 20 mM dNTP mix (Thermo Fisher Scientific), 0.26 µl RNasin ribonuclease inhibitor (Promega), 0.26 µl SuperScript III reverse transcriptase (Thermo Fisher Scientific), and 2.08 µl RNase-free water. The reaction mixture was incubated at 42°C for 1 min followed by 50°C for 1 h. cDNA mixtures were diluted in LOTE buffer (3 mM Tris-HCl (Thermo Fisher Scientific) and 0.2 mM EDTA (Sigma-Aldrich) before storage at −20°C.

qRT-PCR procedure. Transcription levels of target genes were quantified using SYBR Green Real-Time PCR master mix (Thermo Fisher Scientific) and specific primer sequences for amplification (Table 1). cDNA samples were amplified using an Agilent Stratagene Mx3000p under the following conditions: (1) denaturing: 95°C for 10 min; (2) cycling: 45 times through a 95°C denature for 30 s, an annealing temperature for 1 min (primer specific), and an extension of 72°C for 1 min. A melting curve assay after the qRT-PCR amplification consisted of increasing from 55°C, held for 30 s, to 95°C. PCR Miner was used to quantify cycling times, reaction efficiency, and sample variability (Zhao and Fernald, 2005). ß-Actin was chosen as the reference gene for quantification of targeted transcript expression. The standard ΔΔCt method was used to produce fold change in gene expression ($2^{-\Delta\Delta Ct}$), with the adult 8 L group acting as the reference for the calculation of the ΔΔ value.

Oxford Nanopore RNA sequencing procedure. TRIzol-extracted RNA was sequenced using a GridION (Oxford Nanopore Technologies) after processing using the protocol outlined in the Oxford Nanopore Technologies PCR-cDNA

Table 1. Targeted qRT-PCR primer sequences and specifications, including forward and reverse primer sequences, annealing temperature, melting temperature, and expected product sizes for *DIO2, DIO3, OPN5, LHβ, FSHβ, PRL*, and *GH*

Gene	Primer	Annealing temperature (°C)	Melting temperature (°C)	Length (bp)
DIO2	CGCCTACAAGCAGGTCAAAC CACACTTGCCACCAACACTCTT	60	82	242
DIO3	AGGCTCTCTTCCTTCGGGAT TAGCACTTGCTAGGCAGCAC	60	83	180
OPN5	ATGGCATCAGACTGCAACTCC AAGGAACAGTAGCCCAGAACG	60	84	499
LHB	TTTACCGCAGCCCTTTGGGT AGAGCCACGGGTAGGATGACTTT	60	87	125
FSHB	CTGCGGTGACCATCCTGAATCTTT GCTTCCATTGTGACTGAAGGAGCA	62	85	396
PRL	AATGAAACCCCGACCCTGAG CCCCTAGTGCAACTTGAGACC	60	79	630
GH	GCTGCCGAGACATACAAAGAG GAGCTGGGATGGTTTCTGAG	60	81	109
ß-actin	AATCAAGATCATTGCCCCAC TAAGACTGCTGCTGACACC	60	84	114

sequencing barcoding kit (SQK-PCB109). Raw Fast5 reads were base called and demultiplexed using the guppy base caller before removing adapters from reads and filtering long reads (>25 bp) using Porechop and Filtlong, respectively. The parameters for each sequencing assay included running at a voltage of −180 mV for 72 h. Gene transcripts were aligned to a reference *Coturnix japonica* genome (https://www.ncbi.nlm.nih.gov/datasets/genome/GCF_001577835.1/) before using Salmon to quantify transcript expression levels. EdgeR was used to identify differentially expressed genes based on their significance value ($p < 0.01$). For analyses comparing all groups, the adult 8 L group was chosen as the reference for comparison.

Gene ontology. Functional annotation of transcripts identified by Oxford Nanopore RNA sequencing was performed using the Database for Annotation, Visualization and Integrated Discovery (DAVID, Sherman et al., 2022). Significantly differentially expressed transcripts across both photoperiod and age were categorized using the functional annotation chart tool.

Statistical analyses and plots. All raw data are provided in extended data (Extended Data Table 2-1). Two-way ANOVA was conducted on testis length, fat score, and hypothalamic *DIO2* and *DIO3* expression. EdgeR was used to determine statistically significant differentially expressed transcripts in the pituitary gland (Robinson et al., 2010; McCarthy et al., 2012; Chen et al., 2016). For the testis length and fat score measures, the three juvenile females were omitted from the analyses. All plots were created in RStudio (R Core Team, 2013; RStudio Team, 2015) using the ggplot2 package, and figures were created using Adobe Illustrator. For all statistical analyses, a *p*-value of <0.05 [and a false discovery rate (FDR) < 0.2, where applicable] was defined as the statistical cutoff for significance. This FDR significance threshold was determined based on the knowledge that *FSHβ* is significantly upregulated in long day adults.

Results

Short photoperiods induce gonadal and adipose involution in adult and juvenile quail

Two-way ANOVA identified that short photoperiod significantly reduced testis length in adult and juvenile quail (Fig. 1a, Table 2). The accompanying table includes *F*- and *P*- statistics for all two-way ANOVA analyses in both Figures 1 and 3. Adult quail had significantly larger testes compared with juveniles. There was a significant interaction suggesting photoperiod effects were larger in adults compared with juvenile birds. Two females in long photoperiod had large ovaries (0.49 and 0.57 cm), and the single female in short photoperiod had a regressed ovary (0.13 cm); however, it was not possible to collect data regarding follicular development. Short photoperiod also reduced adipose tissue indicated by lower fat scores compared with birds in long photoperiod (Fig. 1b). Juvenile quail had lower fat scores compared with adult birds. There was no significant photoperiod by development interaction. All three juvenile females, omitted from the fat score analyses, had a fat score of 3.

Age-dependent photoperiodic changes in hypothalamic deiodinase expression

Two-way ANOVA identified a significant photoperiod by age interaction for hypothalamic *DIO2* expression (Fig. 1c, Table 2). Overall, there was no significant main effect of photoperiod on *DIO2* expression. There was a significant effect of age on *DIO2* expression. There was a significant interaction for hypothalamic *DIO3* expression (Fig. 1d). There was also a significant main effect of photoperiod and age. These findings suggest that *DIO2* and *DIO3* are highly sensitive to photoperiodic state in adult quail with significantly higher levels in long photoperiod and short photoperiod, respectively. Surprisingly, *DIO2* was observed to be significantly elevated in short photoperiods in juvenile birds. *DIO3* expression levels were similar in both long and short photoperiod conditions.
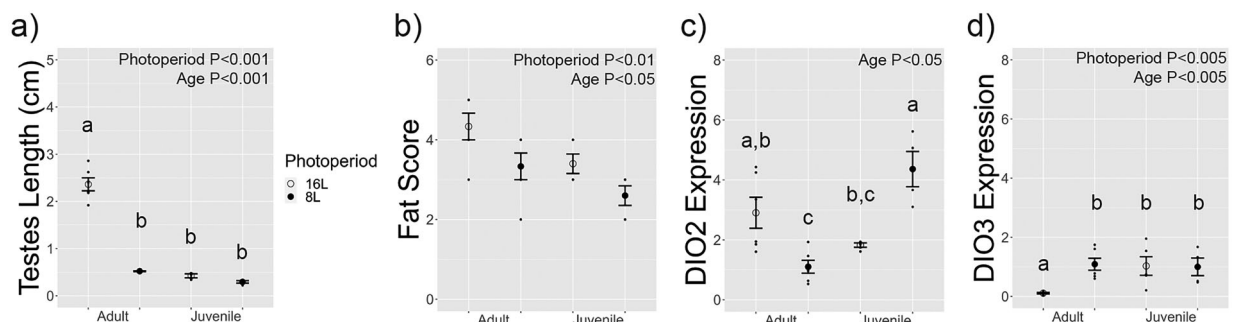

Figure 1. Long photoperiods induce physiological and hypothalamic neuroendocrine change associated with reproduction in adult and juvenile Japanese quail. *a*, Measurements of testis length showed a significant interaction between photoperiod and age. *b*, Fat score ratings, as established by Wingfield and Farner, were overall higher in adults and in 16L photoperiod conditions. *c*, qRT-PCR analyses show a significant photoperiod by age interaction on *DIO2* expression in the MBH. *d*, A significant photoperiod by age interaction was also found in MBH *DIO3* expression. Physiological and transcriptomic data from qRT-PCR were analyzed by two-way ANOVA and Tukey's HSD with an α value of *p* = 0.05. The letters above each group indicate pairwise comparisons by Tukey's HSD where appropriate.

Photoperiod- or developmental-induced changes in transcript expression in the pituitary gland

Our sequencing assays resulted in transcriptomes being produced with an average N50 value of approximately 1 kb and an average depth of 4.53. edgeR analyses identified 206 transcripts that were differentially expressed between long and short photoperiod treatments in adults (Fig. 2a; Extended Data Table 2-1). A total of 126 transcripts were upregulated, and 80 were downregulated in long compared with short photoperiod. As anticipated, $FSH\beta$, prolactin (PRL), and neurotensin (NTS) were found to be differentially expressed between long and short photoperiods in adults. A total of 184 transcripts were differentially expressed between long and short photoperiod treatments in juveniles (Fig. 2b). Forty transcripts were upregulated, and 144 were downregulated in long compared with short photoperiod. HAPLN1 was found to be differentially expressed between long and short photoperiods in juveniles. A total of 685 transcripts were differentially expressed between 16 L adults and 16 L juveniles (Fig. 2c). A total of 175 transcripts were upregulated, and 510 were downregulated. GH was found to be differentially expressed between 16 L adults and 16 L juveniles. A total of 678 transcripts were differentially expressed between 8 L adults and 8 L juveniles (Fig. 2d). A total of 422 transcripts were upregulated, and 156 were downregulated. Again, GH was identified as a differentially expressed transcripts between 8 L adults and 8 L juveniles. edgeR identified that 331 transcripts were differentially expressed across the four treatment groups (Fig. 3a). A heatmap of the top 50 most significantly differentially expressed genes comparing across all four groups (adult and juvenile 8 L and 16 L) was plotted, including $FSH\beta$ and GH (Fig. 3a). PRL, $FSH\beta$, GH, OPN5, NTS, MEF2A, and MEF2D were selected to plot the counts per million for each treatment group (Extended Data Fig. 3-1A–G). Relevant statistics have been provided in the appropriate figure legend.
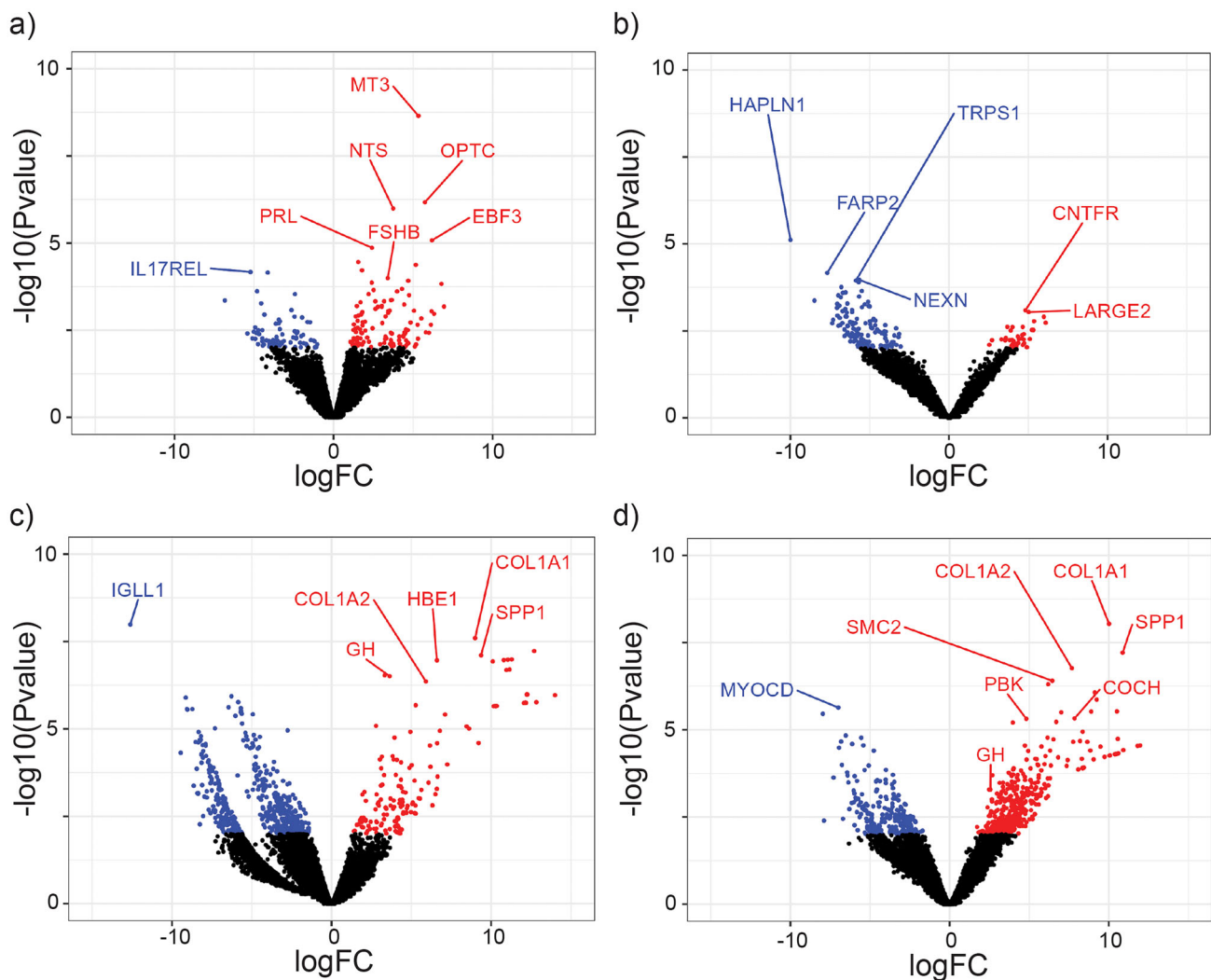

Figure 2. Volcano plots comparing age and photoperiod revealed a high number of differentially expressed transcripts. Upregulated transcripts (logFC > 1) are colored red, and downregulated transcripts (logFC < −1) are colored blue. *a*, Significant differentially expressed transcripts across photoperiod treatments in adults (n = 206) included $FSH\beta$, PRL, and NTS. *b*, Significant differentially expressed transcripts across photoperiod treatments in juveniles (n = 184) included HAPLN1. *c*, Significant differentially expressed transcripts across 16L age groups (n = 685) included GH. *d*, Significant differentially expressed transcripts across 8L age groups (n = 678) also included GH. A *p*-value of <0.01 was deemed significant for all plots.
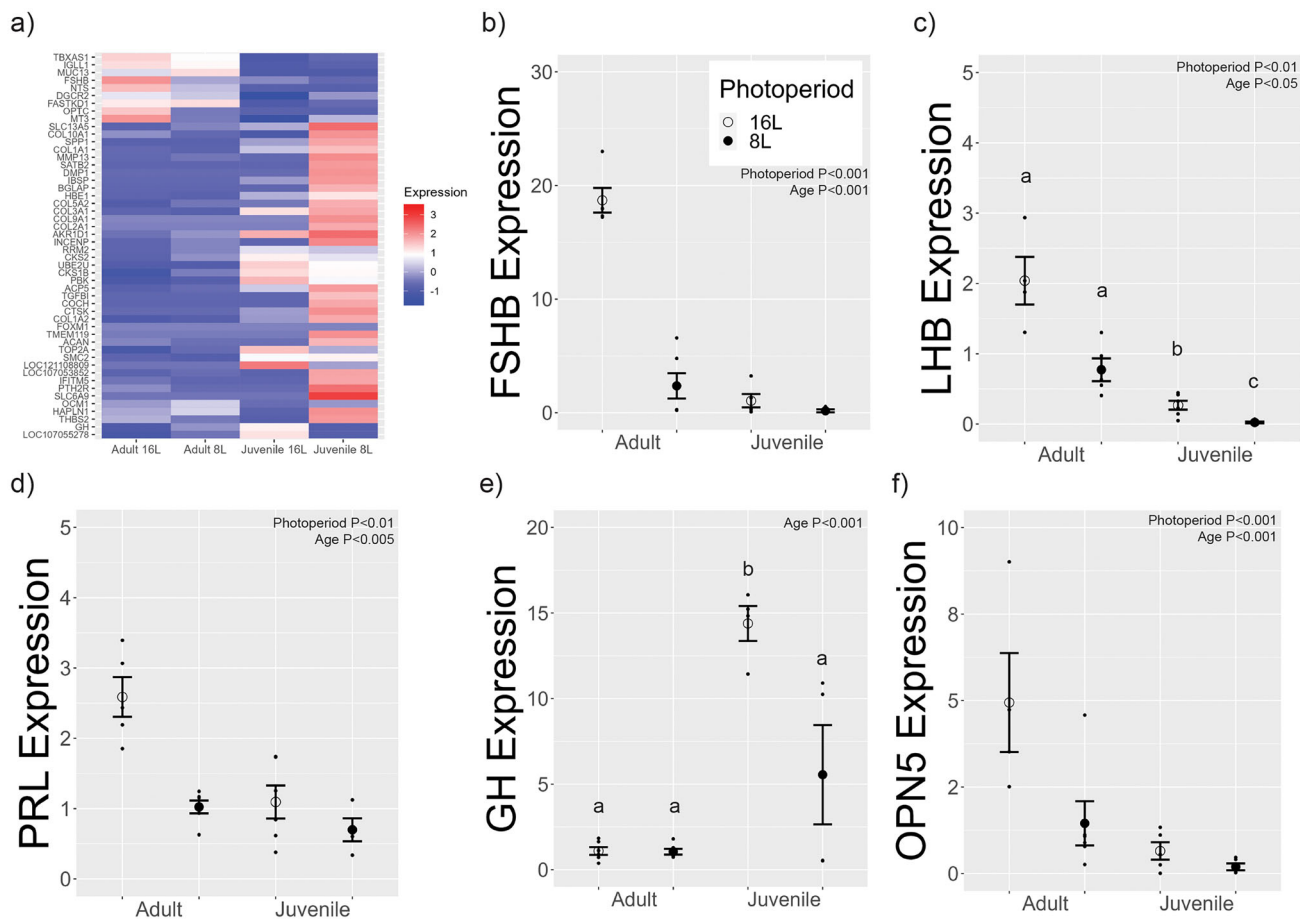
Figure 3. *a*, A heatmap of the top 50 most significant transcripts in the pituitary gland. Among the most significant transcripts were *FSHß* and *GH*. *b–f*, Targeted qRT-PCR analyses were performed in order to investigate the transcription of genes of interest influenced by photoperiod and age. *b–d*, There were significant main effects of both photoperiod and age on *FSHß*, *LHß*, and *PRL* expression, as well as an interaction effect between photoperiod and age on *LHß* expression. *e*, There was a significant photoperiod by age interaction on *GH* expression. *f*, There was a significant main effect of photoperiod and age on *OPN5* expression. For the pituitary sequencing heatmap analysis, a *p*-value of 0.01 was deemed significant. Targeted qRT-PCR analyses were performed using two-way ANOVA and Tukey's HSD with an *α* value of *p* = 0.05. The letters above each group indicate pairwise comparisons by Tukey's HSD where appropriate. Additional data relating to these analyses are provided in Extended Data Figures 3-1 and 3-2.

Table 2. Summary of two-way ANOVA analyses associated with Figures 1 and 3, including *F*- and *P*-statistics associated with the main effects of photoperiod and age, and their interaction, on testis length, fat score, and the expression of *DIO2*, *DIO3*, *FSHβ*, *LHβ*, *PRL*, *GH*, and *OPN5E*

	Photoperiod	Age	Photoperiod:age
Testis length	$F_{(1,15)} = 198.46, p = 4.69 \times 10^{-10}$***	$F_{(1,15)} = 112.75, p = 2.26 \times 10^{-8}$***	$F_{(1,15)} = 81.17, p = 1.94 \times 10^{-7}$***
Fat score	$F_{(1,16)} = 9.23, p = 7.83 \times 10^{-3}$**	$F_{(1,16)} = 6.15, p = 2.46 \times 10^{-2}$*	$F_{(1,16)} = 0.00, p = 1.00$ n.s.
DIO2	$F_{(1,16)} = 0.77, p = 3.94 \times 10^{-1}$ n.s.	$F_{(1,16)} = 6.94, p = 1.81 \times 10^{-2}$*	$F_{(1,16)} = 22.12, p = 2.4 \times 10^{-4}$***
DIO3	$F_{(1,17)} = 10.78, p = 4.38 \times 10^{-3}$**	$F_{(1,17)} = 13.40, p = 1.94 \times 10^{-3}$**	$F_{(1,17)} = 15.30, p = 1.12 \times 10^{-3}$**
FSHβ	$F_{(1,17)} = 17.69, p = 5.95 \times 10^{-4}$***	$F_{(1,17)} = 29.54, p = 4.45 \times 10^{-5}$***	$F_{(1,17)} = 0.83, p = 3.75 \times 10^{-1}$ n.s.
LHβ	$F_{(1,17)} = 9.47, p = 6.83 \times 10^{-3}$**	$F_{(1,17)} = 74.37, p = 1.29 \times 10^{-7}$***	$F_{(1,17)} = 4.68, p = 4.51 \times 10^{-2}$*
PRL	$F_{(1,17)} = 9.27, p = 7.34 \times 10^{-3}$**	$F_{(1,17)} = 14.64, p = 1.35 \times 10^{-3}$**	$F_{(1,17)} = 1.92, p = 1.83 \times 10^{-1}$ n.s.
GH	$F_{(1,16)} = 3.46, p = 8.14 \times 10^{-2}$ n.s.	$F_{(1,16)} = 21.48, p = 2.75 \times 10^{-4}$***	$F_{(1,16)} = 5.67, p = 3.00 \times 10^{-2}$*
OPN5	$F_{(1,16)} = 17.01, p = 7.96 \times 10^{-4}$***	$F_{(1,16)} = 24.79, p = 1.36 \times 10^{-4}$***	$F_{(1,16)} = 0.05, p = 8.21 \times 10^{-1}$ n.s.

Additional data relating to these analyses are provided in Extended Data Tables 2-1–2-3.
Nonsignificant *p*-values are indicated by "n.s.," *p*-values <0.05 are indicated by "*," <0.01 by "**," and <0.001 by "***."

qRT-PCR analyses confirm transcript expression identified in transcriptome analyses

In order to confirm the differential expression, qRT-PCR analyses were performed on select neuroendocrine transcripts of interest including *FSHß*, *LHß*, *PRL*, *GH*, and *OPN5*. There was a significant main effect of photoperiod (Fig. 3*b*, Table 2) and age for *FSHß* expression. There was no significant interaction on *FSHß* expression. These data support the conjecture

that *FSHß* expression is elevated in long photoperiods and is higher in adults. There was a significant photoperiod–age interaction on *LHß* expression (Fig. 3c). There were significant main effects for photoperiod and age on *LHß* expression. There was a significant main effect of photoperiod on *PRL* expression (Fig. 3d) and age. There was no significant photoperiod by age interaction on *PRL* expression. There was a significant photoperiod by age interaction on *GH* expression ($F_{(1,16)} = 5.67$, $p < 0.05$; Fig. 3e). There was a significant main effect of age but not photoperiod on *GH* expression. There was a significant main effect of photoperiod on *OPN5* expression (Fig. 3f) and age. There was no significant photoperiod by age interaction. Overall, transcript analyses using qRT-PCR assay were consistent with the counts per million determined by transcriptome sequencing.

Functional pathways

In order to determine the general functions of significantly differentially expressed transcripts of interest across photoperiod and age, DAVID functional annotation was used (Extended Data Tables 2-2, 2-3, respectively). For these analyses, a *p*-value of <0.05 was used as the significance cutoff. In the comparison between adults and juveniles, the functional groups with the highest significance included those involved in the extracellular matrix (ECM), ECM–receptor interaction, secretion, and focal adhesion. The photoperiod comparison again showed these functional groups as significant and also showed significant transcripts involved in symport, behavior, neuroactive ligand–receptor interaction, and transcription regulation.

Discussion

This study demonstrates that somatotrophs significantly increase *GH* expression during development regardless of the prevailing photoperiod condition. Conversely, lactotrophs and gonadotrophs are primarily sensitive to photoperiod condition with increased *FSHß* and *LHß* expression in long days. Only *LHß* expression was dependent on both photoperiod and developmental condition suggesting this transcript has seasonal- and age-dependent regulation. Despite both adults and juveniles having smaller testes in short photoperiods, there are several transcripts that show developmental- and photoperiod-dependent expression. For example, juvenile quail had 143/144 transcripts upregulated in short photoperiod that were not significantly differentially expressed in adults. Moreover, there were 39/40 transcripts downregulated in juvenile quail without any significant differential expression in adults. Surprisingly, the well-characterized *DIO2* and *DIO3* photoperiodic changes in expression were only identified in adult birds. qRT-PCR analyses confirmed the gene count data identified by RNA sequencing and provided strong internal replication. Overall, these findings indicate a suite of photoperiod-induced molecular changes in the pituitary gland that are age-dependent and a plethora of targets that could help uncover how juveniles have a heightened sensitivity to photoperiod cues compared with adult birds.

Long days facilitate gonadal growth in adults and juveniles

Both adults and juveniles had larger testes in a long photoperiod as opposed to a short photoperiod, consistent with previous publications (Robinson and Follett, 1982). Follett and Farner have previously shown that prolonged exposure of juvenile quail from hatching to long photoperiods can cause increased testis growth (Follett and Farner, 1966). The change in juveniles could be due to two potential mechanisms. First, similar to adults, the photoperiod induces light-dependent changes in gonadal growth. Alternatively, the second mechanism could be due to developmental programs. In hamsters, early exposure to photoperiod or melatonin can delay gonadal growth (Prendergast et al., 2013; Sáenz de Miera et al., 2017). In the current study, it is possible that short photoperiod exposure delayed the developmental program (or puberty) in juvenile quails. This conjecture also applies to the photoperiod-induced changes in fat score. Future analyses of the MBH and pituitary are required to establish the mechanisms upstream of the pituitary that influence photoperiodic and developmental programs in reproduction physiology.

Adult neuroendocrine transcription in the MBH is typical for a long day response

Adult MBH *DIO2* and *DIO3* were increased and decreased in 16 L compared with 8 L respectively, as expected (Yasuo et al., 2005, 2006). We found that juvenile *DIO2* expression increased during short days and that *DIO3* expression did not significantly differ between long and short photoperiods. Given the role of *DIO2* and *DIO3* in the neuroendocrine signal transduction cascade that links photoreception with reproductive physiology (Nakane and Yoshimura, 2010), the dynamics of *DIO2* are surprising. These data appear to suggest that other molecular neuroendocrine changes drive photoperiodic sensitivity in juvenile quail. In juvenile hamsters, *DIO2* has similar levels in long and short photoperiod conditions (Prendergast et al., 2013). *DIO2* expression, leading to a hypothalamic increase in T3, is thought to establish reproductive maturation in mammals. *DIO2* has a wide role in development and has established roles for fisheye metamorphosis and in T3-dependent amphibian metamorphosis (Duarte-Guterman et al., 2010; Itoh et al., 2010). These data indicate that juvenile photoperiodic responsiveness might not be driven by tanycyte rewriting consistent with adult responses. An alternative proposition is other neuronal circuits associated with developmental control of the GnRH system are involved. The stimulation of pituitary cells by GnRH to secrete *LHß* and *FSHß* is partly regulated by the secretion of melatonin in sheep (Misztal et al., 2002). GABA also regulates GnRH neurons independent of the neuroendocrine response to changing

photoperiod (Bentley et al., 2006). Hence, these findings support an alternative means by which pituitary *LHß* secretion may be governed outside of the *DIO2/DIO3*-involved neuroendocrine cascade.

Photoperiod- and age-dependent changes in pituitary gland transcriptomes

Our volcano plot comparing differential expression of adults in long and short photoperiodic conditions revealed a total of 206 differentially expressed transcripts. A total of 126 transcripts were upregulated in a long photoperiod, and 80 were downregulated. Among the differentially expressed transcripts were *PRL*, *FSHß*, and *NTS*. Long photoperiod increases in *PRL* expression, associated with seasonal timing, are common within the literature (Goldsmith and Hall, 1980; Sharp, 2005). Similarly, *FSHß* content increases during long photoperiod conditions (Follett and Maung, 1978; Urbanski and Follett, 1982; Nicholls et al., 1983) where increased FSH in the pituitary gland precedes increases in plasma concentration. Given its role in acting directly on gonads to induce growth, it is not surprising that *FSHß* levels should be high in stimulatory long day photoperiods. *NTS* has a suggested role in regulating *LH* secretion (Rostène and Alexander, 1997). Yamada and Mikami described the distribution of *LH*-releasing hormone (*LHRH*) as coinciding with dense populations of *NTS* when using comparable data between ducks and quail (Yamada and Mikami, 1981). Although *LHß* is absent from the reference *Coturnix japonica* reference genome, and therefore was not identified through RNA sequencing, *LHß* is known to increase in long photoperiod conditions (Follett et al., 1975; Nicholls et al., 1983). Hence, an accompanying increase in *NTS* expression would be expected.

Our volcano plot comparing differential expression across ages in 16 L birds revealed a total of 685 differentially expressed transcripts. A total of 175 transcripts were upregulated in juveniles, and 510 were downregulated. Critically, among the differentially expressed transcripts was *GH*, whose expression is known to be downregulated in adults (Schew et al., 1996). *GH* expression is therefore an excellent marker of age, supporting the significance of the remaining age-dependent differentially expressed transcripts presented here. Similar results were observed in our volcano plot comparing differential expression across ages in 8 L birds. Here, 678 transcripts were differentially expressed, with 422 being upregulated and 156 being downregulated in juveniles. Again, *GH* was one transcript whose upregulation in juveniles was apparent.

Function pathways modified during photoperiod and developmental programming

A functional annotation analysis across photoperiodic conditions suggests an influence of seasonal time on transcripts involved with the brain and nervous system, as neuroactive ligand–receptor interaction scored highly in significance. In both neuroactive ligand–receptor interaction and secretion, *PRL* was identified as a key gene of interest. *FSHß* was also implicated in neuroactive ligand–receptor interaction. Therefore, this analysis confirms the photoperiodic differential expression of these important transcripts that we have focussed on in this manuscript.

The ECM–receptor interaction was identified as the most significant category in our comparison of photoperiodic gene functions. The ECM–receptor interaction is known to play an important role in tissue and organ morphogenesis, including adipogenesis (San et al., 2021). Furthermore, a recent study on the gonadal development of male geese has implicated significant enrichment of the ECM–receptor interaction pathway by differential gene expression in the pituitary gland (Tang et al., 2022). Therefore, the ECM–receptor interaction pathway is a likely area for the identification of photoperiodically significant transcripts. For example, integrin alpha 3 (*ITGA3*) showed significant differential expression within the ECM–receptor interaction pathway and is associated with neural migration. Within this pathway we also identified chondroadherin (*CHAD*), which has a role in mediating the adhesion of chondrocytes; and *COL2A1*, for the production of the pro-alpha1 chain of type-II collagen protein, suggesting that cartilage synthesis is an important physiological change occurring across photoperiodic time.

DAVID functional annotation analyses confirmed that many transcripts, particularly those implicated in growth and development, were differentially expressed across age groups. Transcripts involved in the ECM and ECM–receptor interaction were among the most significant in the functional annotation analysis. The ECM is critical for practically all tissue morphogenesis (Gullberg and Ekblom, 2003), hence why transcripts implicated in its expression are differentially expressed during the rapidly developing juvenile life stage. Furthermore, the TGF-ß signaling pathway was implicated as significant in this analysis. This pathway is thought to be involved in the testicular development of broiler roosters under long (16 L:8 D) photoperiod conditions (Sun et al., 2020) and functions similarly in quail (Otake and Park, 2016).

Similar to the photoperiod comparison, many named transcripts, implicated in the ECM–receptor interaction pathway, were identified in this comparison across age, including *CHAD* and *COL1A2*. Bone morphogenetic proteins 4, 5, and 6 (*BMP4*, *5*, and *6*) were implicated in secretion and differentially expressed between adults and juveniles. It is suggested that *BMPs* may have a role in the multiple craniofacial bone growth of birds; *BMP4* is critical for beak development and is expressed in multiple craniofacial bones of Huiyang bearded chickens, and is therefore likely an important transcript of interest when examining age differences in growth and development of Japanese quail (Hong et al., 2019).

Overall, it is apparent that these functional analyses provide a valuable resource for the identification of novel transcripts associated with both age and photoperiodism. Other groups in the field have used this common method of functional annotation similarly, in order to identify salient areas for future targeted research, for example, in migratory black-headed buntings (Sharma et al., 2018) and Japanese quail (Marasco et al., 2016).

Targeted qRT-PCRs replicate findings obtained through transcriptome analyses

qRT-PCRs for *PRL*, *FSHß*, *LHß*, and *GH* confirm data generated using Oxford Nanopore RNA sequencing. *PRL* is a well-known marker of long photoperiod in birds (Yasuo et al., 2004; Sharp, 2005). qRT-PCR analyses indicate that *PRL* expression is significantly high in the adult 16 L group compared with the 8 L group. Surprisingly, there was a photoperiodic difference in juveniles. In juveniles, the lack of *PRL* change supports the conjecture that light exposure modifies a developmental program similar to the lack of changes observed in the MBH *DIO2/DIO3* system. Similarly, *FSHß* was increased in adults exposed to long photoperiods, consistent with previous reports (Yasuo et al., 2006). However, there was no change observed in the juvenile pituitary gland. *FSHß* causes gonadal cell proliferation and the inhibition of *FSHß* in quail results in the regression of testis size (Brown and Follett, 1977). The lack of a change in *FSHß* in the juveniles suggests that short photoperiod delayed testicular growth. We propose that *PRL* and *FSHß* are molecular markers of photoperiodic programs in adult Japanese quail.

LHß expression, however, was found to increase in both adult and juvenile 16 L conditions (Follett et al., 1975; Nicholls et al., 1983). It is interesting that *LHß* expression is increased in juveniles housed in long photoperiod and indicates that the testicular growth observed was a result of the direct action of *LHß* on the testes. These data indicate that *LHß* expression is under the control of photoperiodic programs in both adult and juvenile quail. It is currently unclear how gonadotrophs that express *LHß* and *FSHß* are differentially regulated by photoperiod and developmental programs, respectively. *OPN5* expression mirrored *LHß* in both adult and juvenile pituitary glands, suggesting a potential molecular mechanism that links light and *LHß* expression, independent of *FSHß* expression.

A clear example of a molecular marker of developmental programs is *GH* expression occurring in somatotrophs. In juvenile quail, there was a robust increase in *GH* expression, independent of photoperiod treatment. Conversely, *GH* expression was found to be consistent across photoperiod conditions in adults. For adults this is expected, as *GH* expression is no longer required for growth and development once maximum size has been reached, and hence ceases to be expressed in older birds (Scanes and Lauterio, 1984). One limitation of the current experiment is the inability to link *GH* expression with body mass.

Conclusions and future research

Overall, the findings reported here indicate pituitary gland cell specificity for photoperiodic and developmental programs of the reproductive physiology of birds. The data indicate somatotrophs as a cellular basis of developmental programs, lactotrophs as a marker of photoperiod programs, and gonadotrophs as a mix of both programs (Extended Data Fig. 3-2); this conclusion builds on recently published work indicating a pituitary cell autonomy, separate from changes driven by the MBH, in seasonal *FSHß* expression (Majumdar et al. 2023). Our approach to conducting Oxford Nanopore RNA sequencing and qRT-PCR analyses to investigate the photoperiodic and developmental responses in quail provides a robust approach to provide a comprehensive and confirmatory strategy. The data generated suggested a wide range of potentially interesting transcripts in the comparisons between photoperiod and age, acting as a resource to guide future research. It is unclear which transcripts and gene ontology pathway analyses are associated with the pituitary cell types. The next steps are to establish which functional pathways are associated with photoperiodic and developmental programs at a cellular resolution. Moreover, many studies have highlighted that photoperiodic cues may be insufficient for full ovarian development indicating that other supplementary cues are required for full reproductive competence (Ball and Ketterson, 2008; Tolla and Stevenson, 2020). Sex differences in the adult and juvenile seasonal programs responses are therefore a salient avenue for future research.

References

Abdelnabi MA, Ottinger MA (2003) Hypothalamic indolamines during embryonic development and effects of steroid exposure. Gen Comp Endocrinol 130:13–19.

Ball GF, Ketterson ED (2008) Sex differences in the response to environmental cues regulating seasonal reproduction in birds. Philos Trans R Soc Lond B Biol Sci 363:231–246.

Barrett P, et al. (2007) Hypothalamic thyroid hormone catabolism acts as a gatekeeper for the seasonal control of body weight and reproduction. Endocrinology 148:3608–3617.

Bentley GE, Kriegsfeld LJ, Osugi T, Ukena K, O'brien S, Perfito N, Moore IT, Tsutsui K, Wingfield JC (2006) Interactions of gonadotropin-releasing hormone (GnRH) and gonadotropin-inhibitory hormone (GnIH) in birds and mammals. J Exp Zool A Comp Exp Biol 305:807–814.

Bradshaw WE, Holzapfel CM (2007) Evolution of animal photoperiodism. Annu Rev Ecol Evol Syst 38:1–25.

Brown NL, Follett BK (1977) Effects of androgens on the testes of intact and hypophysectomized Japanese quail. Gen Comp Endocrinol 33:267–277.

Chen Y, Lun AT, Smyth GK (2016) From reads to genes to pathways: differential expression analysis of RNA-Seq experiments using Rsubread and the edgeR quasi-likelihood pipeline. F1000Res 5:1–48.

Duarte-Guterman P, Langlois VS, Pauli BD, Trudeau VL (2010) Expression and T3 regulation of thyroid hormone-and sex steroid-related genes during *Silurana (Xenopus) tropicalis* early development. Gen Comp Endocrinol 166:428–435.

Follett BK (1976) Plasma follicle-stimulating hormone during photoperiodically induced sexual maturation in male Japanese quail. J Endocrinol 69:117–126.

Follett BK, Farner DS (1966) The effects of the daily photoperiod on gonadal growth, neurohypophysial hormone content, and neurosecretion in the hypothalamo-hypophysial system of the Japanese quail (*Coturnix coturnix japonica*). Gen Comp Endocrinol 7:111–124.

Follett BK, Farner DS, Mattocks PW Jr (1975) Luteinizing hormone in the plasma of white-crowned sparrows (*Zonotrichia leucophrys gambelii*) during artificial photostimulation. Gen Comp Endocrinol 26:126–134.

Follett BK, Maung SL (1978) Rate of testicular maturation, in relation to gonadotrophin and testosterone levels, in quail exposed to various artificial photoperiods and to natural daylengths. J Endocrinol 78:267–280.

Follett BK, Sharp PJ (1969) Circadian rhythmicity in photoperiodically induced gonadotrophin release and gonadal growth in the quail. Nature 223:968–971.

Goldsmith AR, Hall M (1980) Prolactin concentrations in the pituitary gland and plasma of Japanese quail in relation to photoperiodically induced sexual maturation and egg laying. Gen Comp Endocrinol 42:449–454.

Gullberg D, Ekblom P (2003) Extracellular matrix and its receptors during development. Int J Dev Biol 39:845–854.

Hau M (2001) Timing of breeding in variable environments: tropical birds as model systems. Horm Behav 40:281–290.

Hong Y, Pang Y, Zhao H, Chen S, Tan S, Xiang H, Yu H, Li H (2019) The morphology of cross-beaks and BMP4 gene expression in Huiyang bearded chickens. Animals 9:1143.

Itoh K, Watanabe K, Wu X, Suzuki T (2010) Three members of the iodothyronine deiodinase family, dio1, dio2 and dio3, are expressed in spatially and temporally specific patterns during metamorphosis of the flounder, *Paralichthys olivaceus*. Zoolog Sci 27:574–580.

Liddle TA, Stevenson TJ, Majumdar G (2022) Photoperiodic regulation of avian physiology: from external coincidence to seasonal reproduction. J Exp Zool A Ecol Integr Physiol 337:890–901.

Majumdar G, Liddle TA, Stewart C, Marshall CJ, Bain M, Stevenson TJ (2023) FSHβ links photoperiodic signalling to seasonal reproduction in Japanese quail. eLife 12:87751.

Marasco V, Herzyk P, Robinson J, Spencer KA (2016) Pre-and post-natal stress programming: developmental exposure to glucocorticoids causes long-term brain-region specific changes to transcriptome in the precocial Japanese quail. J Neuroendocrinol 28:3955–3964.

McCarthy DJ, Chen Y, Smyth GK (2012) Differential expression analysis of multifactor RNA-Seq experiments with respect to biological variation. Nucleic Acids Res 40:4288–4297.

Misztal T, Romanowicz K, Barcikowski B (2002) Melatonin-a modulator of the GnRH/LH axis in sheep. Reprod Biol 2:267–275.

Nakane Y, Yoshimura T (2010) Deep brain photoreceptors and a seasonal signal transduction cascade in birds. Cell Tissue Res 342:341–344.

Nakane Y, Yoshimura T (2014) Universality and diversity in the signal transduction pathway that regulates seasonal reproduction in vertebrates. Front Neurosci 8:115.

Nakao N, et al. (2008) Thyrotrophin in the pars tuberalis triggers photoperiodic response. Nature 452:317–322.

Nicholls TJ, Follett BK, Robinson JE (1983) A photoperiodic response in gonadectomized Japanese quail exposed to a single long day. J Endocrinol 97:121–126.

Otake S, Park MK (2016) Expressional changes of AMH signaling system in the quail testis induced by photoperiod. Reproduction 152:575–589.

Payton L, Sow M, Massabuau JC, Ciret P, Tran D (2017) How annual course of photoperiod shapes seasonal behavior of diploid and triploid oysters, *Crassostrea gigas*. PLoS One 12:e0185918.

Pérez JH, Tolla E, Bishop VR, Foster RG, Peirson SN, Dunn IC, Meddle SL, Stevenson TJ (2023) Functional inhibition of deep brain non-visual opsins facilitates acute long day induction of reproductive recrudescence in male Japanese quail. Horm Behav 148:105298.

Pérez JH, Tolla E, Dunn IC, Meddle SL, Stevenson TJ (2019) A comparative perspective on extra-retinal photoreception. Trends Endocrinol Metab 30:39–53.

Plant TM (2015) Neuroendocrine control of the onset of puberty. Front Neuroendocrinol 38:73–88.

Prendergast BJ, Hotchkiss AK, Bilbo SD, Nelson RJ (2004) Peripubertal immune challenges attenuate reproductive development in male Siberian hamsters (*Phodopus sungorus*). Biol Reprod 70:813–820.

Prendergast BJ, Pyter LM, Kampf-Lassin A, Patel PN, Stevenson TJ (2013) Rapid induction of hypothalamic iodothyronine deiodinase expression by photoperiod and melatonin in juvenile Siberian hamsters (*Phodopus sungorus*). Endocrinology 154:831–841.

Rani S, Kumar V (2014) Photoperiodic regulation of seasonal reproduction in higher vertebrates.

R Core Team (2013) *A language and environment for statistical computing*. R Foundation for Statistical Computing.

Robinson JE, Follett BK (1982) Photoperiodism in Japanese quail: the termination of seasonal breeding by photorefractoriness. Proc R Soc Lond B Biol Sci 215:95–116.

Robinson MD, McCarthy DJ, Smyth GK (2010) edgeR: a Bioconductor package for differential expression analysis of digital gene expression data. Bioinformatics 26:139–140.

Rostène WH, Alexander MJ (1997) Neurotensin and neuroendocrine regulation. Front Neuroendocrinol 18:115–173.

RStudio Team (2015) *RStudio: integrated development environment for R*, Vol, 14. Boston, MA: RStudio. Inc.

Sáenz de Miera C, Bothorel B, Jaeger C, Simonneaux V, Hazlerigg D (2017) Maternal photoperiod programs hypothalamic thyroid status via the fetal pituitary gland. Proc Natl Acad Sci U S A 114:8408–8413.

San J, Du Y, Wu G, Xu R, Yang J, Hu J (2021) Transcriptome analysis identifies signaling pathways related to meat quality in broiler chickens–the extracellular matrix (ECM) receptor interaction signaling pathway. Poult Sci 100:101135.

Scanes CG, Lauterio TJ (1984) Growth hormone: its physiology and control. J Exp Zool 232:443–452.

Schew WA, McNabb FA, Scanes CG (1996) Comparison of the ontogenesis of thyroid hormones, growth hormone, and insulin-like growth factor-I in ad libitum and food-restricted (altricial) European starlings and (precocial) Japanese Quail. Gen Comp Endocrinol 101:304–316.

Sharma A, Singh D, Das S, Kumar V (2018) Hypothalamic and liver transcriptome from two crucial life-history stages in a migratory songbird. Exp Physiol 103:559–569.

Sharp PJ (1996) Strategies in avian breeding cycles. Anim Reprod Sci 42:505–513.

Sharp PJ (2005) Photoperiodic regulation of seasonal breeding in birds. Ann N Y Acad Sci 1040:189–199.

Sherman BT, Hao M, Qiu J, Jiao X, Baseler MW, Lane HC, Imamichi T, Chang W (2022) DAVID: a web server for functional enrichment analysis and functional annotation of gene lists (2021 update). Nucleic Acids Res 50:216–221.

Spears N, Finley CM, Whaling CS, Tuthill CR, Zucker I (1990) Sustained reproductive responses in Djungarian hamsters (*Phodopus sungorus*) exposed to a single long day. Reproduction 88:635–643.

Stevenson TJ, Ball GF (2012) Disruption of neuropsin mRNA expression via RNA interference facilitates the photoinduced increase in thyrotropin-stimulating subunit β in birds. Eur J Neurosci 36:2859–2865.

Stevenson TJ, Hahn TP, Ball GF (2012a) Variation in gonadotrophin-releasing hormone-1 gene expression in the preoptic area predicts transitions in seasonal reproductive state. J Neuroendocrinol 24:267–274.

Stevenson TJ, Hahn TP, MacDougall-Shackleton SA, Ball GF (2012b) Gonadotropin-releasing hormone plasticity: a comparative perspective. Front Neuroendocrinol 33:287–300.

Stevenson TJ, Liddle TA, Stewart C, Marshall CJ, Majumdar G (2022) Neural programming of seasonal physiology in birds and mammals: a modular perspective. Horm Behav 142:105153.

Stevenson TJ, Prendergast BJ, Nelson RJ (2017) Mammalian seasonal rhythms: behavior and neuroendocrine substrates. In: *Hormones, brain and behavior* (Pfaff DW, Arnold AP, Etgen AM, Fahrback SE, Rubin RT, eds). Columbus: Elsevier Academic Press.

Sun L, Guo L, Wang J, Li M, Appiah MO, Liu H, Zhao J, Yang L, Lsu W (2020) Photoperiodic effect on the testicular transcriptome in broiler roosters. J Anim Physiol Anim Nutr 104:918–927.

Tang B, Hu S, Ouyang Q, Wu T, Lu Y, Hu J, Hu B, Li L, Wang J (2022) Comparative transcriptome analysis identifies crucial candidate

genes and pathways in the hypothalamic-pituitary-gonadal axis during external genitalia development of male geese. BMC Genomics 23:1–12.

Tolla E, Stevenson TJ (2020) Sex differences and the neuroendocrine regulation of seasonal reproduction by supplementary environmental cues. Integr Comp Biol 60:1506–1516.

Urbanski HF, Follett BK (1982) Photoperiodic modulation of gonadotrophin secretion in castrated Japanese quail. J Endocrinol 92:73–83.

Wingfield JC, Farner DS (1978) The endocrinology of a natural breeding population of the white-crowned sparrow (Zonotrichia leucophrys pugetensis). Physiol Zool 51:188–205.

Wood S, Loudon A (2014) Clocks for all seasons: unwinding the roles and mechanisms of circadian and interval timers in the hypothalamus and pituitary. J Endocrinol 222:39–59.

Yamada S, Mikami SI (1981) Immunocytochemical localization of neurotensin-containing neurons in the hypothalamus of the Japanese quail, Coturnix coturnix japonica. Cell Tissue Res 218:29–39.

Yasuo S, Watanabe M, Iigo M, Yamamura T, Nakao N, Takagi T, Ebihara S, Yoshimura T (2006) Molecular mechanism of photoperiodic time measurement in the brain of Japanese quail. Chronobiol Int 23:307–315.

Yasuo S, Watanabe M, Nakao N, Takagi T, Follett BK, Ebihara S, Yoshimura T (2005) The reciprocal switching of two thyroid hormone-activating and -inactivating enzyme genes is involved in the photoperiodic gonadal response of Japanese quail. Endocrinology 146:2551–2554.

Yasuo S, Watanabe M, Tsukada A, Takagi T, Iigo M, Shimada K, Ebihara S, Yoshimura T (2004) Photoinducible phase-specific light induction of Cry1 gene in the pars tuberalis of Japanese quail. Endocrinology 145:1612–1616.

Yoshimura T, Yasuo S, Watanabe M, Iigo M, Yamamura T, Hirunagi K, Ebihara S (2003) Light-induced hormone conversion of T4 to T3 regulates photoperiodic response of gonads in birds. Nature 426:178–181.

Zhao S, Fernald RD (2005) Comprehensive algorithm for quantitative real-time polymerase chain reaction. J Comput Biol 12:1047–1064.